Defect production and lifetime control in electron and γ-irradiated silicon

S. D. Brotherton and P. Bradley
Philips Research Laboratories, Redhill, Surrey, RH1 5HA, England

(Received 14 December 1981; accepted for publication 2 April 1982)

A study of the effect of 1- and 12-MeV electron and Co^{60} γ irradiation has been made on power *p-i-n* diodes and Schottky barrier diodes fabricated on the same starting material. A comparison of the results from these two types of structures illustrated the influence of device processing on the type of defects formed by subsequent irradiation. Detailed electrical characterization of the defects demonstrated good consistency between certain elements of the structural nature of the defect, inferred from these measurements, and those already obtained from electron spin resonance (ESR) measurements. Lifetime measurements on the *p-i-n* diodes indicated that both the *A* center and the divacancy were active recombination centers. Finally, data are presented on defect and lifetime annealing.

PACS numbers: 71.55.Fr, 72.20.Jv, 61.80.Ed, 61.80.Fe

I. INTRODUCTION

In recent years interest has developed in the application of high-energy electron and γ irradiation for recombination lifetime control in silicon.[1-4] The major advantages of this technique over the more conventional process involving metallic diffusions (such as gold or platinum) are the reproducibility of the dose, the opportunity to kill lifetime at the end of all high-temperature processing (such that batch to batch variation in unkilled lifetime can be taken into account), and the means of tailoring lifetime after killing by annealing at temperatures around 300 °C.

However, in spite of the available published material on radiation effects in silicon, there are still areas of uncertainty when applying the techniques to power devices fabricated on float-zoned substrates. For instance, much of the early work of Watkins, Corbett, and Walker[5-7] employed Czochralski material and electron doses greater than would be envisaged for power-device lifetime control. Similarly, the electrical characterization of the defects in *n*-type silicon reported by Kimerling[8] was carried out mainly on Czochralski substrates. Although Evwaraye and Baliga[3] have studied the defects produced in *p-i-n* diodes fabricated on float-zoned substrates, no information was given in that work on the effects of the diode fabrication schedule itself. Moreover, there is still a lack of agreement in the published work on the identification of the center responsible for lifetime control, with both the *A* center[9] (oxygen-vacancy complex) and the divacancy[3] being cited.

In the work presented below, some of these problems have been addressed; in particular, the influence of the irradiation conditions on recombination lifetime has been examined, and it is demonstrated that neither the *A*-center nor the divacancy alone is responsible for lifetime control, but both centers are involved in parallel.

An examination was also made of the influence of the power-device processing schedule on the defects formed, and it was concluded that the major effect of the processing schedule was to increase the level of oxygen in the material which thereby resulted in the suppression of certain irradiation-induced defects.

Finally, results are presented on the annealing characteristics of the defects.

The irradiations used in this work were 1- and 12-MeV electrons and γ rays from a Co^{60} source.

The sample preparation and the irradiation conditions are described in Sec. II, the characterization of the irradiation-induced defects is presented in Sec. III, and the lifetime and annealing results are contained within Secs. IV and V, respectively.

II. SAMPLE PREPARATION AND IRRADIATIONS

Most of the samples used in this study were fabricated upon $\sim$60-Ω cm neutron-transmutation doped (NTD) float-zoned *n*-type silicon. The two device structures used were commercial *p-i-n* power diodes and aluminum Schottky barrier diodes fabricated upon otherwise unprocessed material. Comparison of the results from these two sample types was used to monitor the effect of power-device processing on defect formation. Schottky barrier samples were also fabricated on 50–100 Ω cm *n*-type Czochralski substrates; differences seen between these samples and the Schottky barrier diodes made on the float-zoned substrates were attributed to oxygen.

The *p-i-n* diodes had deep diffused n^+ and p^+ regions of 73 and 47 μm depths, respectively. The n^- base width was nominally 85 μm. The formation of the deep n^+ and p^+ regions necessitated diffusion times of approximately 25 h at temperatures in excess of 1200 °C in oxygen. The oxygen solubility in silicon at these temperatures is $\sim 10^{18}$ cm^{-3},[10] and from the published diffusion coefficients[11] and standard diffusion theory,[12] it can be shown that the oxygen content in the middle of a 205-μm thick slice will be $5\text{–}6\times 10^{17}$ cm^{-3}. In other words, at the end of the diode fabrication schedule, the original float-zoned material looked more like Czochralski material so far as its oxygen content was concerned. Evidence of the increased oxygen concentration in these samples was provided by detection of the oxygen thermal donor[13] which had been formed by a low-temperature anneal at the end of the diode fabrication schedule. The donor density in the base of these devices, as measured by *C-V*

 0021-8979/82/085720-13$02.40

profiling, was found to be 1.4×10^{14} cm^{-3}, compared with 8.3×10^{13} cm^{-3} in the Schottky barrier samples. The deep level transient spectroscopy (DLTS) spectra obtained from these unirradiated samples are shown in Fig. 1; the large low-temperature peak, observed only in the *p-i-n* diode, is attributed to the oxygen thermal donor level. These measurements confirmed the expectation that the *p-i-n* diode fabrication schedule had significantly changed the character of the substrate material, both in terms of its oxygen content and the net doping level.

The samples were irradiated after all high-temperature processing had been completed and any processing necessary after irradiation, such as lithography and mounting and bonding, was performed without raising the sample temperature above room temperature.

The electron irradiations were carried out at 1 and 12 MeV. The 1-MeV irradiations were performed at AEG Telefunken in Hamburg at a dose rate of 2 μA/cm^2, with the samples mounted on a water-cooled tray.

The 12-MeV irradiations were carried out at the Instrument Research Technology Corporation (IRT) San Diego, U.S.A., using a high-dose rate pulsed beam which was rastered and at the M. E. L. Equipment Co. Ltd. (MEL), Crawley, England, using a modified Philips SL75/20 linear accelerator which gave a uniform beam over an area of 20×20 cm^2. A low-dose rate of 80 krads/min was employed with this machine. The purpose of this comparison was to assess the importance of the dose-rate characteristics. Very little difference was seen between the samples irradiated in the two different machines. At both MEL and IRT the machine operators provided dosimetry, but calibrated dyed perspex dosimeters[14] were also included with the silicon samples to provide a cross check on doses received from the different machines. A plot of requested dose (in electrons per square centimeter) against measured dose (in megarads from dyed perspex dosimeters) is given in Fig. 2(a) for the samples irradiated at IRT. Reasonable linearity between the two is seen except for the lowest dose and a conversion factor of 4.35×10^{13} electrons/cm^2/Mrad is obtained from these data. This factor was used to convert the doses given to the MEL irradiated samples from megarads to electrons per square centimeter.

A comparison of the doses registered by the perspex dosimeters and an *in situ* ionization gauge used for the irradiations at MEL is shown in Fig. 2(b). Reasonable linearity is seen between these measurements, confirming the reliability

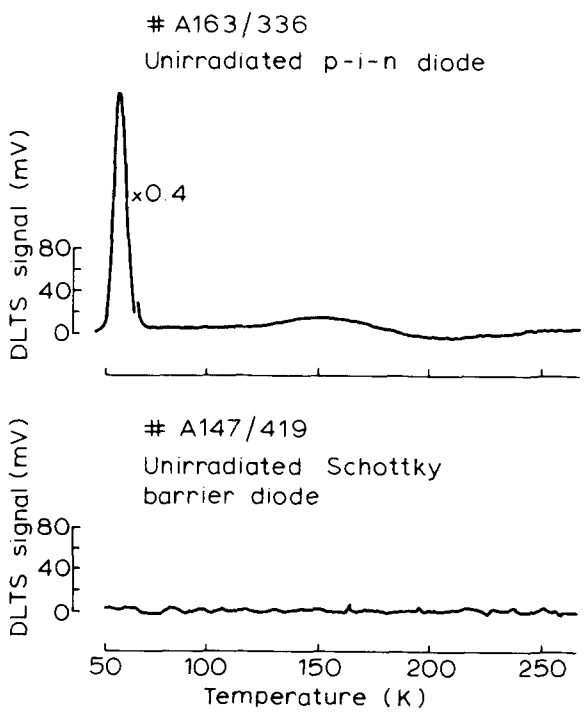

FIG. 1. DLTS plots obtained from unirradiated Schottky barrier and *p-i-n* diodes (τ = 14 ms).

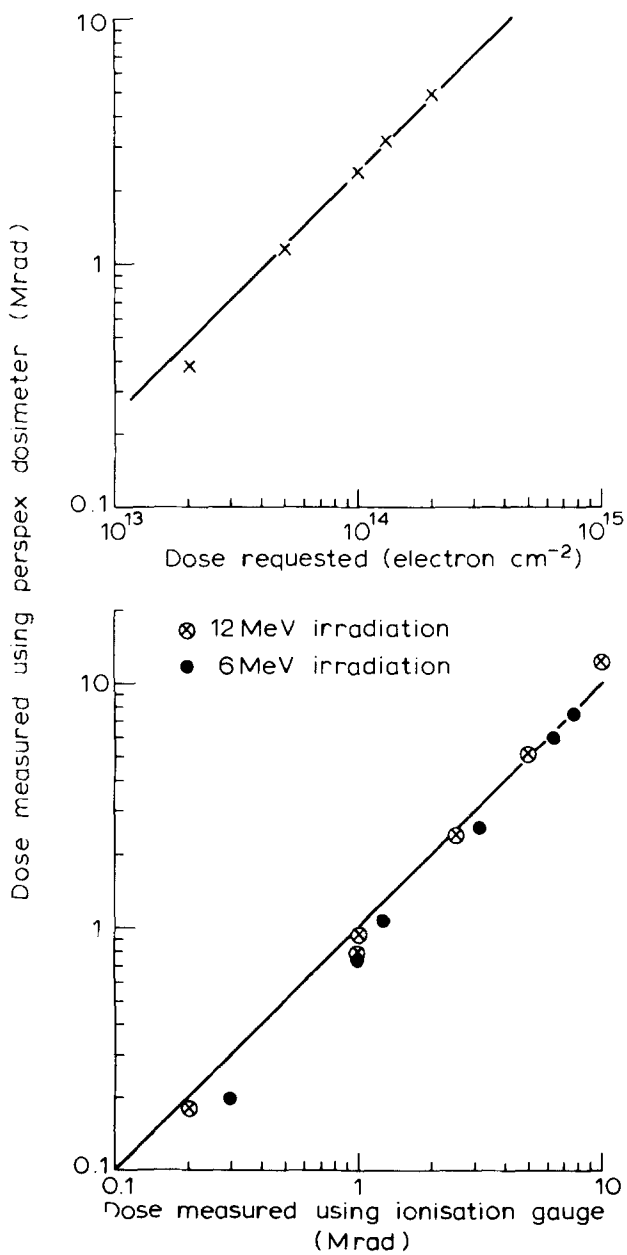

FIG. 2. (a) Electron dose measured using dyed perspex dosimeters as a function of requested dose in electron/cm^2 (12-MeV irradiations at IRT, San Diego). (b) Comparison of dose measurements using dyed perspex dosimeters and *in situ* ionization gauge (12-MeV irradiations at MEL, Crawley).

of the dyed perspex dosimeters.

The γ irradiations were obtained from a Co^{60} source at Salford University, England. The agreement between the doses quoted by them and those measured with the perspex dosimeters was poor, with the perspex dosimeters indicating a dose at least 50% larger than quoted. For this reason the γ irradiation doses quoted need to be treated with caution.

III. DEFECT FORMATION AND CHARACTERIZATION

The point defects formed by the irradiations were electrically characterized using DLTS[15] and also by detailed measurements of electron capture and emission rates under constant capacitance conditions at stabilized temperatures with temperature stability of better than ± 0.15 K during the measurement.

A. Defect formation

In order to examine the dependence of defect formation on device processing, the results obtained from the *p-i-n* diodes were compared with data from Schottky barrier diodes made on unprocessed slices. The differences between two such types of devices are illustrated in Fig. 3; this displays the DLTS spectra obtained from two samples irradiated at 1 MeV with 2.2×10^{14} e/cm^2. Major differences are readily apparent between these two samples, with the *p-i-n* diode displaying the low-temperature oxygen-donor peak 4 as well as smaller-magnitude peaks 1 and 3. These differences are discussed in more detail in the following sections.

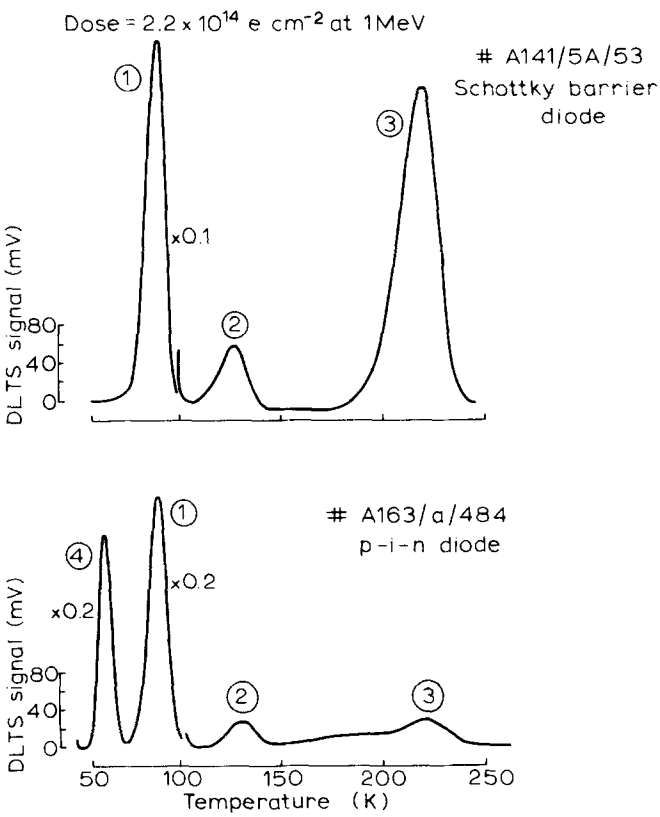

FIG. 3. DLTS plots of electron-irradiated Schottky barrier and *p-i-n* diodes. Electron dose = 2.2×10^{14} cm^{-2} at 1 MeV (τ = 14 ms).

1. DLTS peak 1

Thermal emission-rate measurements made on peak 1 in both the Schottky barrier sample and the *p-i-n* diode sample gave an activation energy of 0.17 eV as shown by the results in Fig. 4. This is the activation energy reported for the *A* center,[5] and in view of this identification, it was unexpected to find that the concentration of centers having this activation energy in the low-oxygen-content Schottky barrier sample was approximately twice the concentration detected in the oxygen-rich *p-i-n* sample. However, electron capture-rate measurements on the Schottky barrier sample revealed the presence of two levels having markedly different capture rates but indistinguishable emission rates. Approximately 50% of the traps at level 1 in the Schottky barrier samples had a fast capture rate and a temperature-independent capture cross section of $1.0\pm0.1\times10^{-14}$ cm^2 (59–92 K); the remaining traps had a very much smaller cross section which decreased with decreasing temperature. The variation of this cross section with temperature over the range 59–92 K is shown in Fig. 5 (line 1). This small value of cross section and its dependence on temperature would suggest that the electron-capture process was onto a negatively charged acceptor level. The capture cross section appears to be thermally activated and, from the limited number of points in Fig. 5, an activation energy of 0.08 ± 0.015 eV was obtained. This leads to an expression for σ_n of

$$\sigma_n = 5\times10^{-13}\exp-(0.08/kT)\text{cm}^2,$$

with at least an order of magnitude uncertainty in the pre-exponential term due to scatter in the experimental points.

Correcting the thermal activation energy of 0.17 eV by the temperature dependence of the capture cross section gave an enthalpy of 0.09 ± 0.015 eV for the slow trapping center in the Schottky barrier diode samples. No such correction was required for the fast trapping level insofar as its

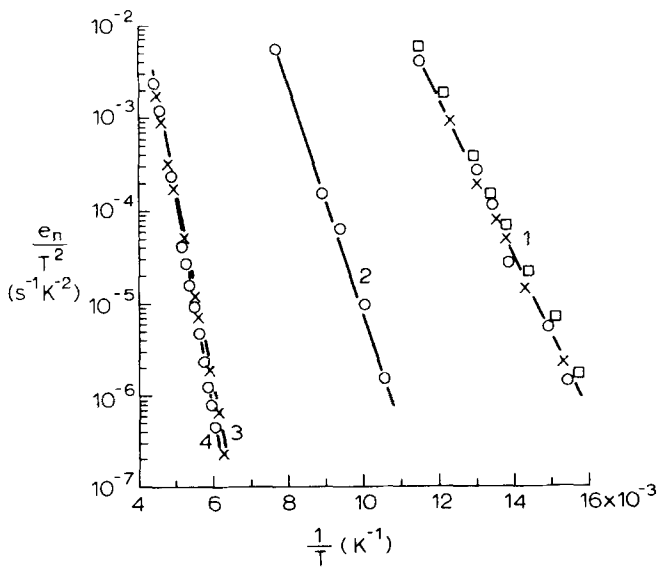

FIG. 4. Thermal emission-rate measurements made on electron irradiation-induced trapping levels. Line 1: *A* center, $E_c - 0.169$ eV. X = *p-i-n* diode, O = Schottky barrier diode after removal of slow trapping level; □ = unannealed Schottky diode. Line 2: Divacancy, $E_c - 0.246$ eV. Line 3: Divacancy, $E_c - 0.413$ eV. Line 4: *E* center, $E_c - 0.456$ eV.

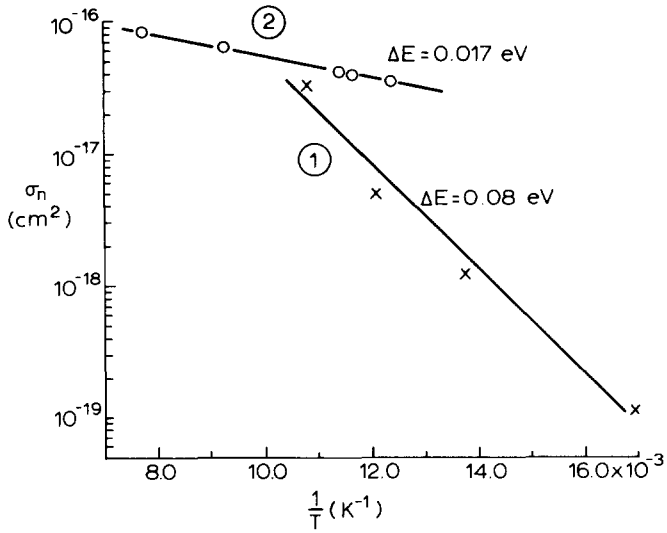

FIG. 5. Temperature dependence of electron-capture cross section of (1) slow trapping level at $E_c - 0.09$ eV and (2) divacancy at $E_c - 0.23$ eV.

electron-capture cross section was independent of temperature. Therefore its enthalpy is 0.17 eV, and this fast trapping center is assumed to be the A center. Examination of the electron-capture rate onto level 1 in the *p-i-n* samples revealed a concentration of the slow trapping level which was about one order less than in the Schottky samples. The majority of the traps at level 1 in the *p-i-n* samples had the same capture cross section (1.0×10^{-14} cm^2) as the fast trapping centers in the Schottky samples. Therefore almost all the defects giving rise to peak 1 in the *p-i-n* sample are assumed to be A centers. Additional justification of this identification is obtained by noting that Kimerling's measurement[8] of the electron-capture cross of the A center is similar to the value quoted above.

Further confirmation of the presence of another level, in addition to the A center, in the Schottky samples was established by annealing one of these samples at 277 °C for 4.5 h, after which time the slow trapping level had been completely removed with very little reduction in the concentration of the fast trapping level. Thermal-emission results obtained from this Schottky barrier sample are shown in Fig. 4. Just a small difference is seen between these data and that obtained in the presence of the slow trapping level. The presence of the $E_c - 0.09$-eV level was not found to be a function of irradiation energy; the only factor determining its presence appeared to be the oxygen content of the material as shown by the results in Table I. These data demonstrate a comparably low concentration of this center in Czochralski silicon to that found in the *p-i-n* structures fabricated on float-zoned silicon. Hence the occurrence of the $E_c - 0.09$-eV center is correlated with the absence of high oxygen concentrations in the material. Moreover, it is related to the primary defect (the vacancy/interstitial pair) since its concentration relative to the A center is not a function of electron-irradiation energy (in contrast to the divacancy). Finally, as demonstrated in Table I, it is not a shallower level associated with the E center, since removal of this center caused no change in the concentration of the $E_c - 0.09$-eV center.

TABLE I. Ratio of concentrations of fast and slow trapping defects having a thermal activation energy of 0.17 eV.

Sample type	Irradiation energy (MeV)	$\frac{N_T(\text{slow})}{N_T(\text{fast})}$	Comments
SB[a]/FZ[b]	1	1.1	
SB/FZ	12	1.2	E center removed
p-i-n/FZ	1	0.1	
SB/CZ[c]	12	<0.1	
SB/CZ + 450 °C	12	0	preirradiation formation of SiO_4 donor complexes
SB/FZ + 450 °C	12	1.1	

[a] SB = Schottky barrier diode.
[b] FZ = Float zoned.
[c] CZ = Czochralski.

This center, whose appearance is indistinguishable from the A center in normal DLTS measurements, would appear to be a dominant defect level in irradiated low-oxygen-content material. In such material it is produced in addition to, not instead of, the A center, and the A-center concentration itself was found to be the same in both the low- and the high-oxygen-content samples (the Czochralski material and the processed float-zoned material). This would appear to be in contradiction with ESR results,[5] but the doses used in that work were orders of magnitude larger than here, and the A-center concentration in their low-oxygen-content material could have saturated at a value well below that measured in their Czochralski material. In addition, the phosphorus concentration in this material was up to two orders of magnitude larger than in the typical power-device material used in the present work, and the competitive trapping of vacancies by the phosphorus could also have contributed to the low concentration of A centers observed.

The identity of the level at $E_c - 0.09$ eV is not obvious, as it does not correlate with any previously reported defect levels. Both Kimerling[8] and Watkins *et al.*[16] have reported states in apparently this position after low-temperature irradiations, but their activation energies of 0.09 eV were, in fact, thermal-activation energies uncorrected for any temperature dependence of the capture cross section. In addition, these levels were reported to anneal out well below room temperature. Therefore these levels must be different from those reported here.

2. DLTS peak 3

A larger-magnitude peak, 3, was observed in all the Schottky barrier samples (e.g., Fig. 3) compared with the *p-i-n* samples. As with peak 1, this is believed to be due to the presence of two separate centers in the Schottky barrier sample giving rise to the single peak. The two centers are believed to be the E center (phosphorus-vacancy complex) and the divacancy. Confirmation of the presence of the E center was obtained by postirradiation annealing of the Schottky barrier sample at 150 °C for 30 min, after which the height of

peak 3 was reduced to a level comparable to peak 2 (as in the *p-i-n* sample). The suggested reason for the much lower concentration of the *E* center in the *p-i-n* sample is that the oxygen (present in higher concentrations) acts as a competing trap for vacancies or even as a recombination center for vacancy/interstitial pairs and suppresses the formation of the vacancy-related *E* center. Confirmation that this effect was due to the incorporation of oxygen into the *p-i-n* diode, and not to some other aspect of the processing, was established by noting the same effect in Schottky barrier diodes fabricated upon unprocessed Czochralski silicon. A similar difference in *E*-center concentrations between high resistivity FZ and CZ silicon has been reported by Kimerling.[8]

3. DLTS peak 2

The DLTS peak 2 in Figs. 3(a) and 3(b) is taken to be the second level of the divacancy in the upper half of the band gap. The equality of peak height for peaks 2 and 3 will be noted in the *p-i-n* sample and, as discussed above, the deeper divacancy level is present, in addition to the *E* center, in peak 3 in the Schottky barrier sample.

The detailed electrical characteristics of these centers are discussed further in Sec. III B.

4. Irradiation energy effects and defect introduction rates

Similar results to those shown in Fig. 3 were obtained from electron irradiations at 12 MeV and also from Co^{60} γ irradiations. The major difference between these irradiations was in the relative concentrations of the *A* center and the divacancy as illustrated in Fig. 6. The smaller number of divacancies produced per *A* center with the γ irradiation is consistent with the higher-energy threshold required for divacancy production.[7] The maximum energy released to a Compton electron by a γ photon is 1.1 MeV, so it is not surprising that, in terms of defect production, the characteristics of γ irradiation are similar to what might be expected from an electron flux of energy somewhat less than 1 MeV.

The defect introduction rates produced by 1 and 12 MeV electron irradiations are summarized in Table II. The introduction rates for the *A* center and divacancy are in agreement with other published data[7,8,17] to a factor of 2 or better. The introduction rates are shown as constant, although the data did indicate a tendency for the rate to decrease with increasing dose up to maximum doses of 5.5×10^{14} electrons/cm^2; however, a more extensive data base would be required to clarify this point.

B. Defect characterization

The thermal emission-rate measurements made on the *A* center, the *E* center, and the two divacancy levels are shown in Fig. 4, and the thermal-activation energies are summarized in Table III. Also contained in this table are the electron-capture cross-section values of which all, except the shallower divacancy level, were independent of temperature. This temperature independence of electron capture onto neutral acceptor levels has previously been reported for gold[18] and platinum[19] in silicon and would appear to be a characteristic of electron capture onto neutral centers in silicon. In contrast, the shallower divacancy center, displaying a temperature-dependent capture cross section (shown as line 2 in Fig. 5) is believed to be capturing an electron onto a negatively charged center. The larger electron-capture cross section at the higher temperatures is taken to be a manifestation of the increased probability of electrons, possessing greater thermal energy, surmounting the repulsive barrier associated with the electron and the negatively charged center. (Finally, it is worth noting that where the interaction between the electron and the center has been attractive, e.g., S^{+} [20,21] and Se^{+} [22] in silicon, the capture cross section has been found to decrease with increasing temperature suggesting a cascade process.)

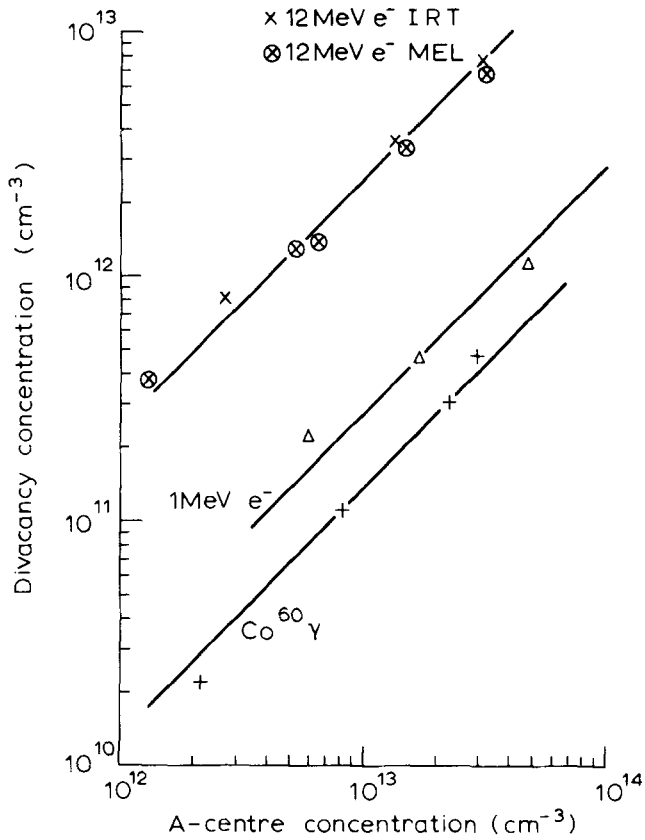

FIG. 6. Relative *A*-center and divacancy concentrations measured in *p-i-n* diodes after irradiations of different energies.

The capture cross-section values, together with the values previously reported for gold[18] and platinum,[19] are plotted as a function of the trap enthalpy in Fig. 7. With the possible exception of the *E* center, a continuous reduction in the value of the electron-capture cross section with trap depth is seen for neutral-acceptor centers in silicon. This trend has been previously described by Lowther[23] as indicative of a multiphonon emission capture process in which the probability of capture diminishes with the increasing number of phonons required to be emitted for deeper traps. The shallower divacancy at $E_c - 0.23$ eV is seen to be two orders of magnitude below the line in Fig. 7, and this small value of the electron-capture cross section, for such a shallow level, is taken as further confirmation of the level being negatively charged before electron capture.

The electron-capture cross section and trap enthalpy

TABLE II. Introduction rates for A center, E center, and divacancy.

Sample type	Irradiation energy (MeV)	Defect introduction rate $\eta(=N_T/\phi)$, (cm^{-1})		
		A center	Divacancy	E center
SB[a]/FZ	1	$7.0 \pm 1 \times 10^{-2}$	$2.3 \pm 0.3 \times 10^{-3}$	$1.5 \pm 0.2 \times 10^{-2}$
p-i-n/FZ	1	$7.7 \pm 0.4 \times 10^{-2}$	$2.3 \pm 0.3 \times 10^{-3}$	5×10^{-4}
SB/FZ	12	0.15 ± 0.02	$4.5 \pm 0.4 \times 10^{-2}$	$3.7 \pm 0.3 \times 10^{-2}$
SB/CZ	12	0.13 ± 0.02	$4.4 \pm 0.4 \times 10^{-2}$	$1.3 \pm 0.3 \times 10^{-2}$
p-i-n/FZ	12	0.14 ± 0.02	$4.0 \pm 0.5 \times 10^{-2}$	$1.0 \pm 0.2 \times 10^{-2}$

[a]SB = Schottky barrier diode, FZ = Float zoned, and CZ = Czochralski.
Note: Dose range = 2×10^{13}–5.5×10^{14} e/cm^2.

values listed in Table III are related to the thermal emission-rate measurements in Fig. 4 by the equation of detailed balance[24,25]:

$$e_n = X_n \sigma_n \langle V \rangle N_c \exp \frac{-\Delta H}{kT}, \quad (1)$$

where ΔH is the trap enthalpy and X_n is related to the total entropy change ΔS_T on ionization of the trap by

$$X_n = \exp \frac{\Delta S_T}{k}.$$

Splitting this into configurational and vibrational components[23]

$$\Delta S_T = k \ln g + \Delta S_{\text{Vib}},$$

where g is the normal degeneracy factor ratio and ΔS_{Vib} is the vibrational entropy change. Hence

$$X_n = g \exp \frac{\Delta S_{\text{Vib}}}{k}.$$

The vibrational entropy change is expected to be close to zero for electron transitions between one antibonding state and another and close to band gap entropy for transitions between bonding states and the antibonding states of the conduction band.[23]

Contained in Table III are values of X_n (expt) calculated from the experimental data by substituting the measured values of e_n, σ_n, and ΔH into Eq. (1). ESR data have indicated that the electron trapping states are antibonding levels for the A center[6] and for the two upper divacancy levels.[26] Hence, the expected values of $X_{n(\text{theor})}$ are as shown in the table (assuming that $g = 1/2$ for states containing 0/1 electrons and 2 for 1/2 electrons). Reasonable agreement is seen between the experimental and theoretical values of X_n for the A center and the deeper divacancy, but in the case of the shallower divacancy level with a fully occupied antibonding state there is a marked discrepancy. The reason for this is not presently understood. The ESR data recorded for the neutral state of the E center[27] identified the site of the signal as being a dangling bond on the silicon atom adjacent to the vacancy. Assuming that this center is essentially antibonding in character, then the expected value of $X_{n(\text{theor})}$ for the E center would be 2, in reasonable agreement with the experimentally determined value of 1.7 listed in Table III.

IV. RECOMBINATION LIFETIME CONTROL

In the currently published work, the center responsible for lifetime control has not been unambiguously established: in two recent studies the conclusion drawn in one case was that the divacancy was the dominant center[3] and in the other the A center was cited.[9] In both cases only one irradiation energy was used. In the results presented below, it is shown that by examining lifetime as a function of divacancy concentration with a varying background concentration of A centers and vice versa (obtained by using two or more irradiation conditions) this point can be more rigorously investigated.

Lifetime related measurements were made on the p-i-n diodes using the diode switching transient waveform[28] and the plateau width t_s was used in particular. This value can be converted into base lifetime[29] although some care is required in ascribing too much meaning to this value when shallow recombination centers are present, which may result in a spatially varying lifetime through the base.[30]

TABLE III. Electrical parameters of radiation-induced deep levels.

Trap	Activation energy[a] (eV)	Capture cross section (cm^2)	Enthalpy (eV)	X_n (expt)	X_n (theor)
A center	0.169	$1.0 \pm 0.1 \times 10^{-14}$	0.169	0.4	0.5
Divacancy	0.413	$2.0 \pm 0.2 \times 10^{-15}$	0.413	0.3	0.5
	0.246	$4 \times 10^{-16} \exp -\frac{0.017}{kT}$	0.230	8	2.0
E center	0.456	$3.7 \pm 0.2 \times 10^{-15}$	0.456	1.7	

[a]Activation energy was obtained from slope of $\ln(e_n/T^2)$ vs $1/T$.

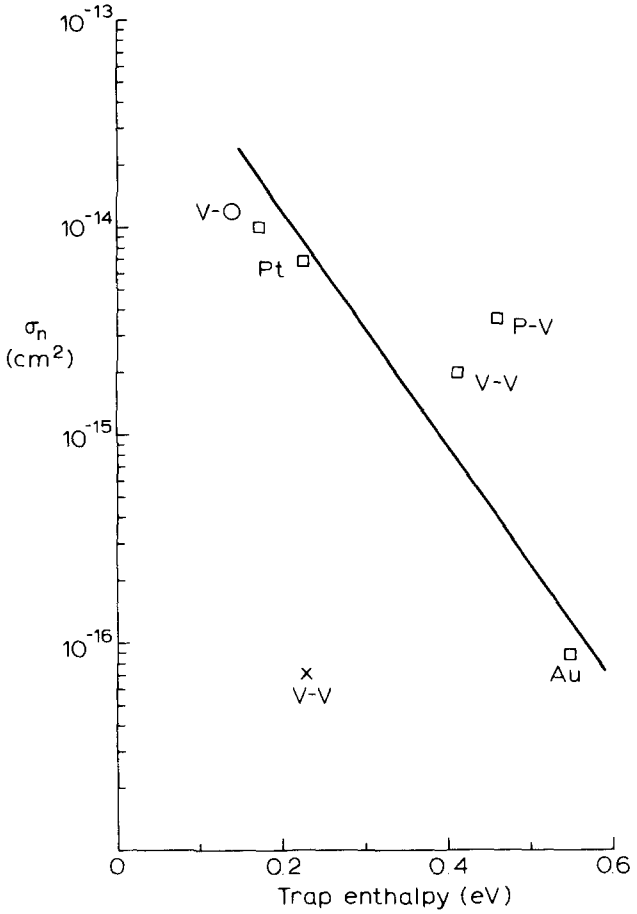

FIG. 7. Observed variation of electron-capture cross section with trap enthalpy for selected centers in the upper half of the silicon band gap.

In investigating the dominant recombination center, the unconverted values of diode plateau width t_s or storage time have been used and were measured with equal forward and reverse currents of 2 A/cm^2.

The dependence of storage time (corrected for the control value) on divacancy concentration for 1- and 12-MeV electron-irradiated and γ-irradiated samples is shown in Fig. 8(a). A similar plot of storage time against A-center concentration is shown in Fig. 8(b). From these figures it is clear that neither the A center nor the divacancy alone can be responsible for lifetime control. It is more likely that both are efficient recombination centers; inspection of Table III shows that, although the A center is considerably shallower than than the deeper divacancy level, its electron-capture cross section is appreciably larger. The shallower divacancy level at $E_c - 0.246$ eV is unlikely to be an effective recombination center because of its small electron-capture cross section.

As mentioned above, it is likely that both the A center and the divacancy participate in recombination and, by taking a linear combination of the two (assuming that they act in parallel), the corrected storage time can be empirically represented by

$$\frac{1}{t_s} = AN_A + BN_{V-V},$$

where $A = 1.27\times10^{-7}$ cm^3 s^{-1} and $B = 5.04\times10^{-7}$ cm^3 s^{-1}.

A plot of the corrected storage time t_s against $AN_A + BN_{V-V}$ is shown in Fig. 9 and it will be seen that all the data points now fall upon a common curve.

In addition to the identification of the recombination centers, a further point of practical importance is the change of lifetime with dose. This is usually described through the lifetime degradation factor k which is defined by

$$\frac{1}{\tau} = 1/\tau_c + k\phi,$$

where τ_c is lifetime before irradiation, τ is lifetime after irradiation, and ϕ is the irradiation fluence in electrons/cm^2 (or Mrads for γ irradiation).

The values of effective base lifetime (so called because the lifetime may not have a single unique value in the base) were extracted from the above mentioned 2-A/cm^2 diode switching data and used to calculate the lifetime degradation factor for 1- and 12-MeV electron irradiations as shown in Fig. 10.

A number of points emerge from this figure:

(i) The results from the 12-MeV irradiations performed with a rastered pulsed beam at IRT and a diffuse large area uniform beam at MEL are virtually identical showing that the lifetime changes caused by the irradiation are largely insensitive to the irradiation technique and to the details of the instantaneous dose rate.

(ii) Published lifetime degradation factors of Carlson *et al.*[2] are 1.2×10^{-8} cm^2/s for 12-MeV irradiations and 3×10^{-10} cm^2/s for 1-MeV irradiations. The 12-MeV results

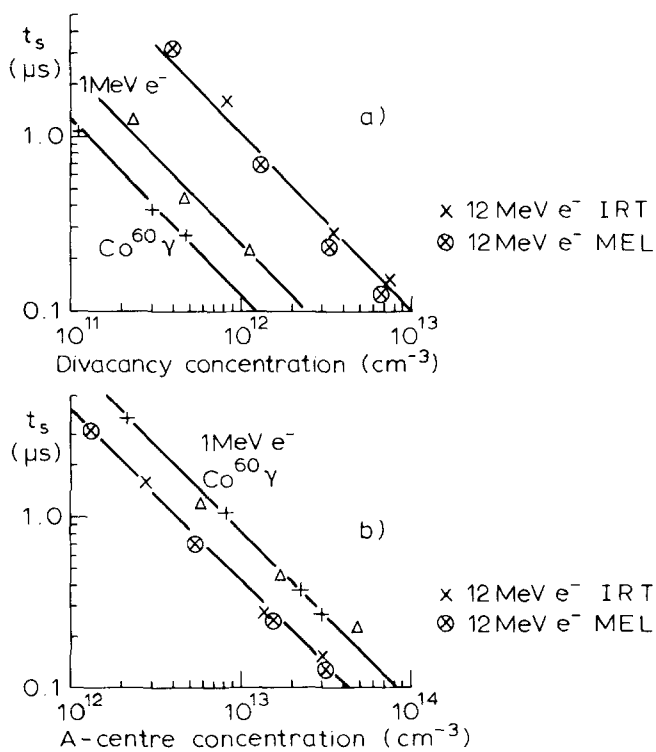

FIG. 8. (a) Diode storage time as a function of divacancy concentration. (b) Diode storage time as a function of A-center concentration (storage time measured with equal forward and reverse current densities of 2 A/cm^2).

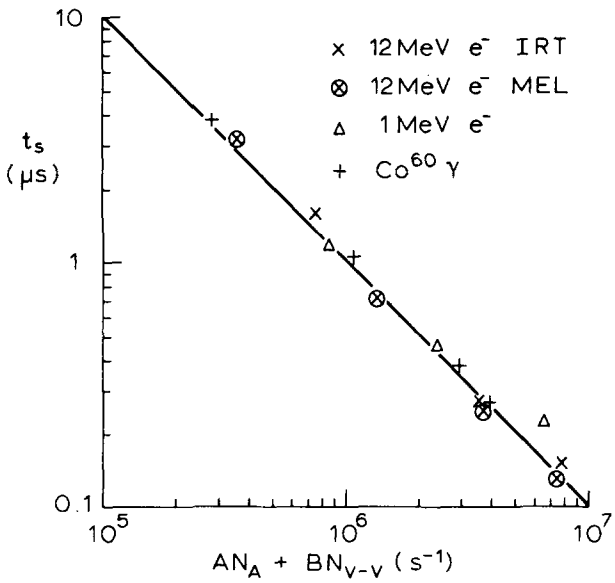

FIG. 9. Diode storage time as a function of the weighted sum of the A-center and divacancy concentrations.

are in good agreement with the points in Fig. 10, but there is a significant difference in the 1-MeV results. A substrate doping dependence of the degradation factor has been reported by Carlson *et al.*,[2] but the magnitude of this effect does not seem large enough to reconcile the results. A degradation factor of 3.4×10^{-9} cm^2/s has been found for 1.5-MeV irradiations of 25–35 Ω cm substrates by Evwaraye and Baliga,[3] which is considerably larger than the value quoted by Carlson *et al.*[2] for similar irradiations. It would appear that presently unidentified factors may be contributing to the variability of the lower-energy electron-irradiation results.

(iii) The lifetime degradation factor is seen to be a function of dose. Two possible reasons may be advanced for this: firstly, as mentioned earlier, the defect introduction rates gave the appearance of decreasing with dose and, secondly, such an effect could be expected to arise from the presence of a shallow recombination center such as the A center. For a shallow recombination center in the upper half of the band gap, the lifetime in a p-i-n diode will be a function of the local excess carrier density Δn:

$$\tau = \tau_{p0}\left(1 + \frac{n_1}{\Delta n}\right) + \tau_{n0}\,, \tag{2}$$

where

$$\Delta n \gg n_0\,,$$

and

$$n_1 = N_c \exp - \frac{(E_C - E_T)}{kT}\,,$$

and for a given forward current density J_F, the mean excess injected carrier density is given by

$$\Delta\bar{n} = \frac{J_F\tau}{qW}, \tag{3}$$

where W is the base width.

Hence on increasing the irradiation dose, the lifetime will inevitably decrease; at the same time, for a given forward current density, there will be a consequent decrease in the steady state injected free carrier density [Eq. (3)]. Through Eq. (2) this will have the effect of reducing the efficiency of the shallow recombination center. Hence the reduction in lifetime with increasing dose will be smaller than anticipated if these effects are ignored. These qualitative arguments have been verified by using a numerical model[29] which simulates the diode switching transient. The model has been used to calculate a lifetime degradation factor ($1/\tau_{\text{eff}}\,N_T$) as a function of recombination center density N_T, where the recombination center has been set at $E_c - 0.17$ eV. The results of this calculation are presented in Fig. 11, and it will be noted that the degradation factor displays behavior which is qualitatively similar to that demonstrated by the experimental results in Fig. 10. The modeled results show a more rapid dropoff of degradation factor with recombination center

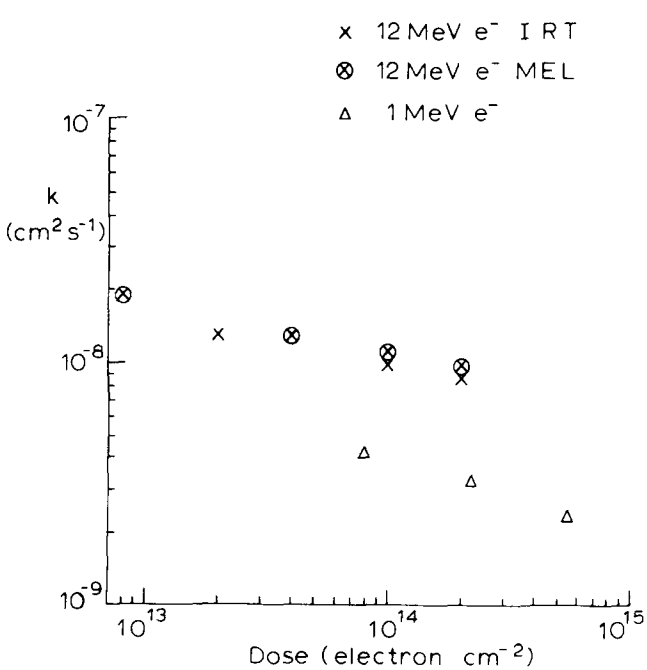

FIG. 10. Lifetime degradation factor variation with electron dose.

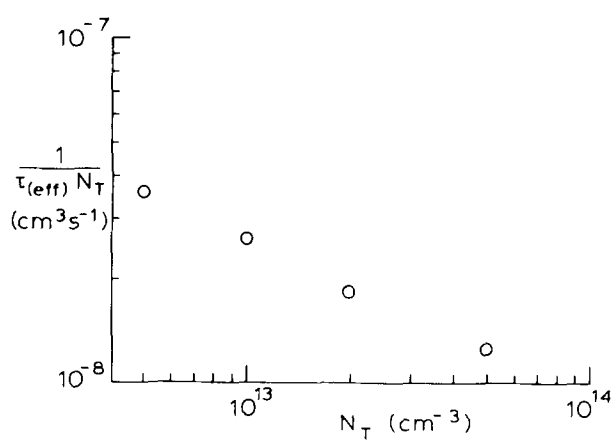

FIG. 11. Modeled variation of effective lifetime degradation factor with recombination center density at $E_c - 0.17$ eV. ($J_R = J_F = 4$ A/cm^2).

density than is displayed in the experimental results. This is because in the model the shallow level at 0.17 eV is the only recombination center, whereas in the experimental samples there is the deeper divacancy recombination level whose efficiency is not expected to be a function of dose.

The dependence of the lifetime degradation factor on dose for the γ-irradiated samples had a similar overall appearance to the electron irradiation results in Fig. 10, with the degradation factor decreasing with increasing dose. The mean value of degradation factor was $5\ s^{-1}\ Mrad^{-1}$, which is approximately an order of magnitude larger than the value quoted by Carlson *et al.*[2] as it was for the 1-MeV electron irradiations. The assumed inaccuracies in dose measurement are clearly not sufficient to account for this difference. It is possible that there are some significant but unidentified material differences between the substrates used in this work and those used by Carlson *et al.*[2]; indeed, degradation factors differing by more than an order of magnitude have been quoted by Lugakov *et al.*[31] for Co^{60} γ irradiations on float-zoned and Czochralski substrates.

V. POSTIRRADIATION ANNEALING

A. Isochronal annealing

A broad picture of the annealing phenomena was obtained from a series of 30-min isochronal anneals with the samples taken to successively higher temperatures for each anneal. The switching time was measured with the *p-i-n* diodes, and the defect density was measured in these diodes as well as in the Schottky diodes.

The results of this study are shown in Fig. 12. The defect annealing results in this figure are broadly similar to those published by Kimerling.[8] The points of general interest in this figure are:

(i) The annealing of the *E* center in the Schottky barrier samples at ~ 150 °C. As discussed in Sec. III A, there was much lower *E*-center production in the *p-i-n* diodes.

(ii) The diode storage time was independent of annealing temperatures below ~ 300 °C, even though appreciable annealing of the divacancy had occurred. At first sight this would appear to be in contradiction to the results discussed in Sec. IV, which suggested that the *A* center and the divacancy controlled lifetime. However, the explanation for this effect is that, during the period when the divacancy was being annealed out, a new center was being annealed in, which was an efficient recombination center. Only when this center and the *A* center started to disappear did the storage time start to increase.

(iii) The divacancy annealed out at lower temperatures in the *p-i-n* sample than in the Schottky sample; this is believed to be due to the presence of excess oxygen in the former acting as a trap for vacancies.[26]

(iv) The *A* center annealed out more quickly in the Schottky barrier samples than in the *p-i-n* samples.

(v) A new defect level was observed to form during the annealing of both types of device. As indicated by the different energy levels and electron-capture cross sections, these two defects were quite different. This difference is discussed further in Sec. V B.

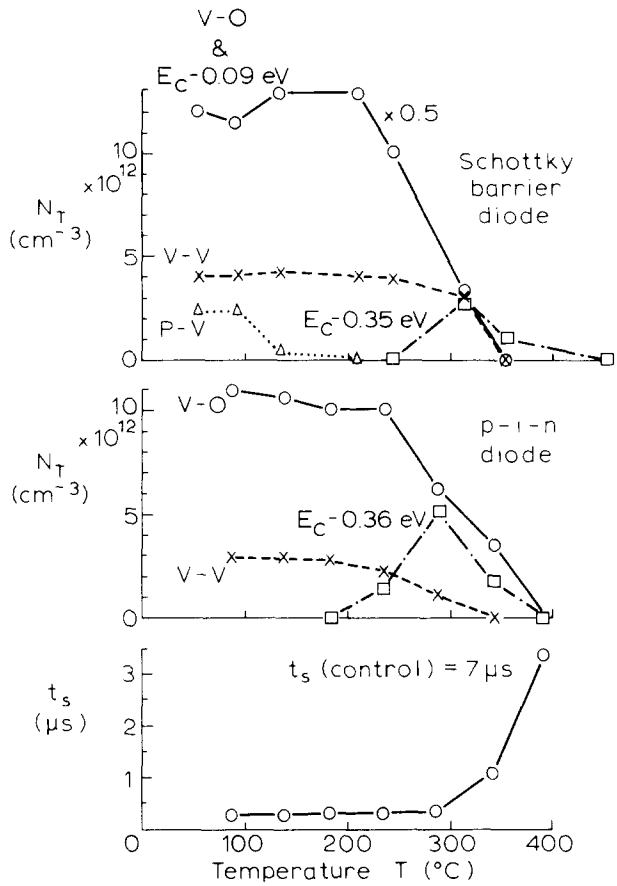

FIG. 12. Effects of 30-min isochronal anneals on lifetime and trap concentrations in 12-MeV irradiated samples. (Annealing induced centers: $E_c - 0.363$ eV, $\sigma_n = 1.4\times 10^{-15}$ cm^2, $E_c - 0.346$ eV, $\sigma_n = 4.6\times 10^{-17}$ cm^2.)

B. Isothermal annealing

Although the results in Fig. 12 give a broad picture of the annealing events, no detailed rate information which can be used to predict device stability is obtained from this type of study. To obtain this information, a series of isothermal anneals was effected over the temperature range from 277 to 356 °C, with annealing time ranging from 0.5 to 24 h. The results revealed by this study were of considerable complexity, in that individual defect annealing processes were only infrequently observed to be through simple first-order reactions, and the rates, moreover, were frequently a function of both the sample type and the irradiation energy. Furthermore, a variety of centers were observed to anneal in, some of which appeared to be close in energy to the center annealing out. This apparent change in energy level of the center with annealing led, in some cases, to ambiguity in the assessment of the concentration of centers remaining after a given anneal. In view of this multiplicity of effects, only the major features will be presented here.

1. Lifetime

The variation of base lifetime with annealing time at 335 °C is illustrated in Fig. 13 for 1- and 12-MeV irradiated samples. As is clear from this figure, the results cannot be described by a single annealing rate constant—no doubt, due to the contribution to lifetime control from two or more

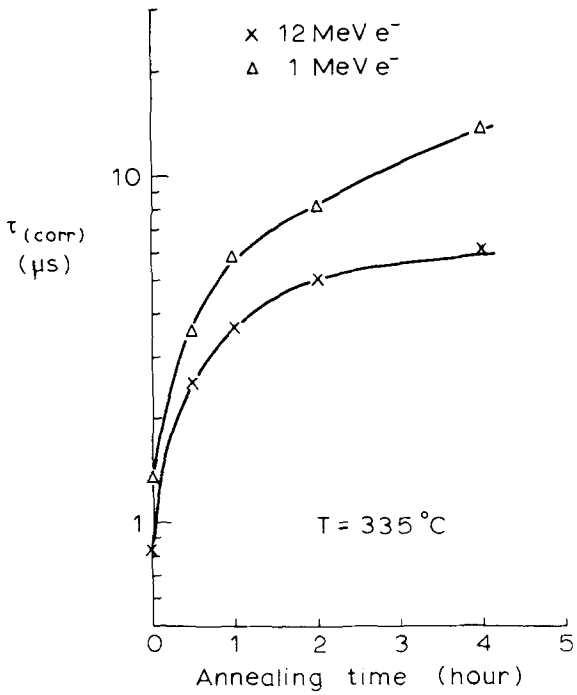

FIG. 13. Variation of recombination lifetime with duration of anneal at 335 °C.

sources. In view of this, an empirical approach was taken to characterize the change of lifetime with annealing. In particular, the time taken for the initial value of irradiation-induced lifetime to double was extracted from the data, and this is plotted in Fig. 14 as a function of temperature. A clear thermal activation is seen from this figure, with broadly similar activation energies for both the 1- and 12-MeV irradiated samples, but with the 1-MeV samples displaying the greater longevity. The results can be represented by

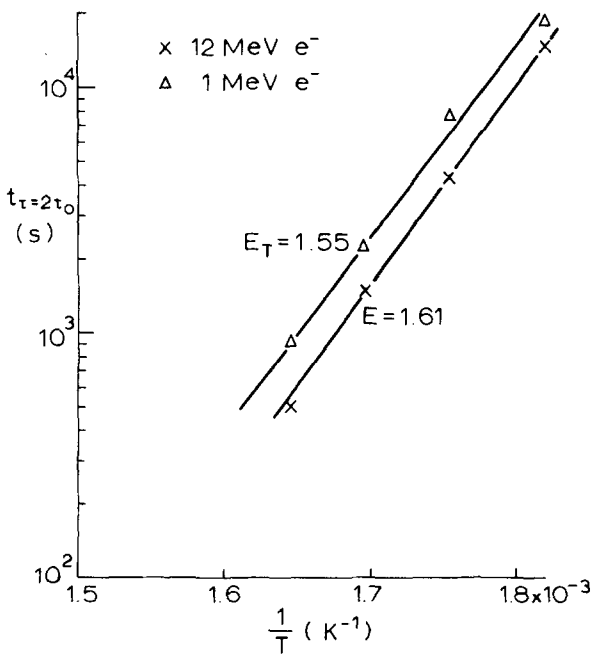

FIG. 14. Activation-energy plot for lifetime change with annealing temperature ($t_{\tau=2\tau_0}$ is time taken for irradiation-associated component of recombination lifetime to double).

$$t_{(\tau=2\tau_0)} = A \exp \frac{E}{kT},$$

where $E = 1.55$ eV, $A = 1.3\times10^{-10}$ s for 1-MeV irradiations, and $E = 1.61$ eV, $A = 2.6\times10^{-11}$ s for 12-MeV irradiations.

Within the scatter of the results in Fig. 14, the quoted differences in activation energy are not regarded as significant. However, the faster overall rate of lifetime change in the 12-MeV irradiated samples is believed to be real and is mainly accounted for by a faster initial change of lifetime with annealing. This is possibly due to the annealing of the divacancy which made a larger proportionate contribution to lifetime in the 12-MeV samples, and, as shown in Fig. 12, the divacancy annealed out more rapidly than the A center.

2. Defect annealing

The data presented below were obtained from a sequential series of DLTS measurements and anneals, relying upon DLTS peak position to identify the various defect levels.

a. A center. A set of annealing data on the A center, obtained after annealing at 317 °C is shown in Fig. 15. This figure illustrates the major features observed with this center:

(a) The annealing rate, after the initial fast change in concentration, was significantly slower in the *p-i-n* diodes than in the Schottky samples.

(b) No significant differences were noted in annealing behavior with irradiation energy.

(c) The annealing kinetics of the *p-i-n* samples were not first order, but gave the appearance of being a two-stage pro-

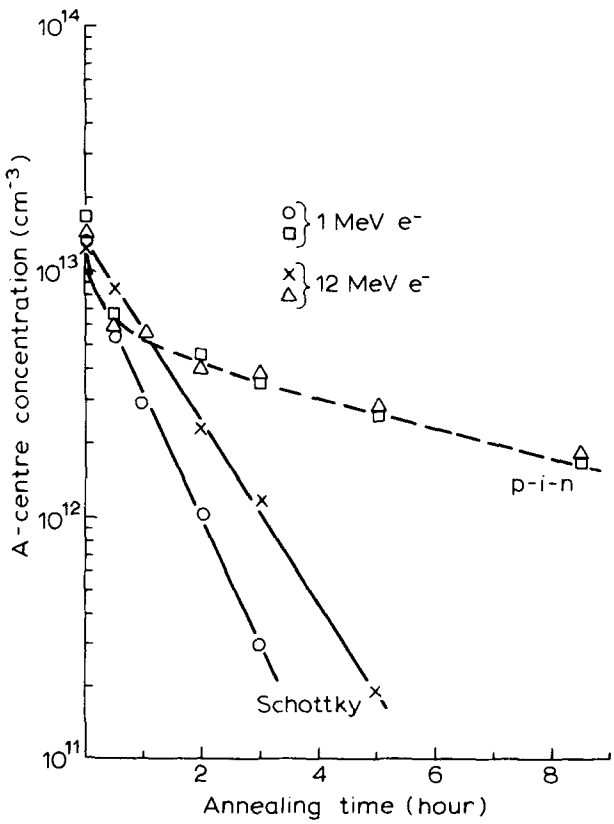

FIG. 15. Variation of A-center concentration with annealing time at 317 °C.

cess. Also, in these samples another center appeared in high concentration after the initial half-hour anneal, whose presence could be correlated with the A center. This was established by noting that the ratio of the concentrations of the new center in the 1- and 12-MeV irradiated samples was 1.1, and the A-center ratio was also 1.1 (the divacancy ratio was 0.1). This center, with a thermal activation energy of 0.363 eV, measured with respect to the conduction band edge and an electron-capture cross section of 1.4×10^{-15} cm^2, was not observed in the Schottky samples. It is possible that the Schottky results illustrate the direct annealing out of the A center, whereas in the *p-i-n* samples the anneal is rate limited through the intermediate stage of another complex. This difference in annealing is almost certainly due to the extra processing which the *p-i-n* samples had. However, it does not simply appear to be the increased oxygen content which is responsible for this effect (as it was with the defect creation discussed in Sec. III A), since Schottky barrier diodes fabricated on Czochralski silicon did not display the rapid formation of the $E_c - 0.363$-eV level which was observed after annealing the *p-i-n* diodes.

The temperature dependence of the time constant of the A-center anneal in the *p-i-n* samples is given by

$$\frac{1}{\tau} = 5.6\times10^{9}\exp-\frac{1.7}{kT}\,\mathrm{s}^{-1}.$$

This was obtained from the slow portion of the annealing data and, as mentioned above, may not represent the intrinsic anneal of the A center but its removal via a two-stage anneal.

If the annealing data observed with the Schottky barrier diodes are taken as the anneal of the A center through a first-order process, then the temperature dependence of the time constant (obtained from only three data points) is given by

$$\frac{1}{\tau} = 3.6\times10^{14}\exp-\frac{2.1}{kT}\,\mathrm{s}^{-1}.$$

This activation energy is considerably larger than has been quoted for the anneal of any other radiation-induced defect in silicon (e.g., divacancy or E center), while for the A center itself very little published information on isothermal annealing is available, apart from a brief reference by Kimerling[8] quoting the annealing time constant to be given by

$$\frac{1}{\tau} = 10^{8}\exp-\frac{1.3}{kT}\,\mathrm{s}^{-1}.$$

This expression is substantially different from that given above; in Fig. 16, both expressions are compared with the original A-center isochronal annealing data of Corbett *et al.*[32] illustrating that the larger activation-energy expression gives at least as good a fit, if not better, to these data. It will be noticed that neither expression is consistent with the extensive tail in the experimental data extending up to 500 °C. This persistence of the A center at annealing temperatures above 400 °C has not been observed in our own experimental work.

b. Divacancy. The annealing characteristics of the divacancy varied both with sample preparation and, rather more unexpectedly, with the electron irradiation energy. In general, the Schottky diodes displayed first order annealing with

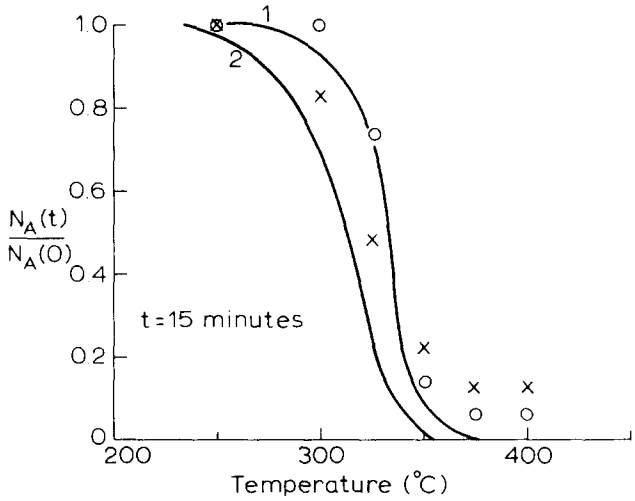

FIG. 16. Comparison of published A-center isochronal annealing data, obtained from ESR and optical absorption measurements, Ref. 32, with calculated isochronal annealing curves using (1) $1/\tau = 3.6\times10^{14}\exp-(2.1/kT)$ reported in the present work and (2) $1/\tau = 10^{8}\exp-(1.3/kT)$ of Ref. 8.

a faster annealing rate for the 1-MeV irradiated samples as shown in Fig. 17. The scatter in the data precluded an accurate assessment of the activation energy for annealing, but indicated an approximate value of 1.3 ± 0.3 eV for both the 1- and 12-MeV irradiated samples. In spite of the reaction appearing to be first order in the Schottky diodes, another center at $E_c - 0.346$ eV with an electron-capture cross section of 4.6×10^{-17} cm^2 annealed into these diodes, which is

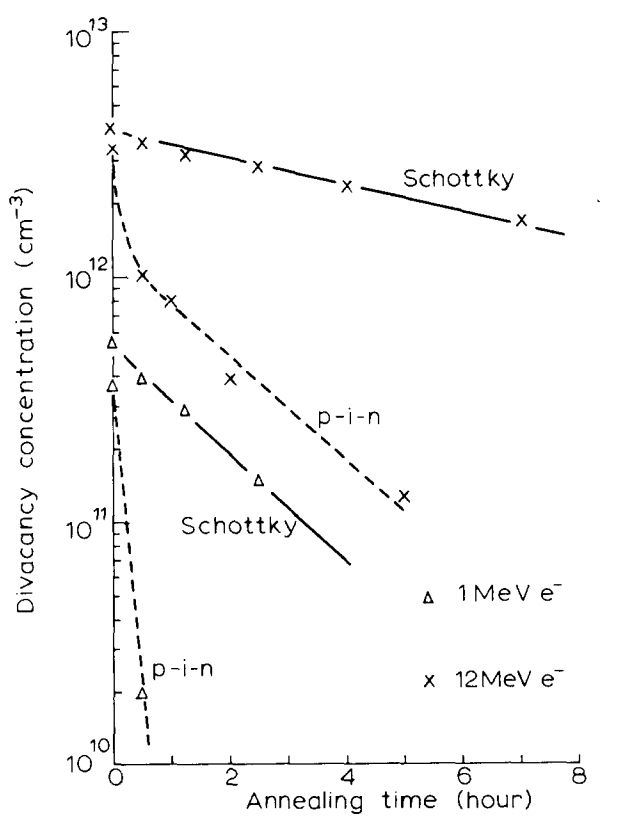

FIG. 17. Comparison of divacancy annealing in *p-i-n* and Schottky barrier diodes at 297 °C.

believed to be divacancy related. This conclusion was drawn from the fact that the concentration ratio of the divacancies in the 1- and 12-MeV irradiated samples was 0.12, and the concentration ratio of the annealing induced centers was 0.1. In contrast, the corresponding A-center ratio was 1.1. The center at $E_c - 0.346$ eV was not observed in the p-i-n diodes; as mentioned earlier, the major annealing induced defect to be observed in these samples was at $E_c - 0.363$ eV, with a significantly larger electron-capture cross section and with quite different annealing-in characteristics.

The p-i-n diodes displayed a divacancy annealing rate which was irradiation-energy dependent (like the Schottky samples), and the rates themselves were significantly faster than observed in the Schottky samples, as illustrated by the data in Fig. 17. Moreover, the annealing of the 12-MeV irradiated p-i-n diodes did not appear to be by a first-order reaction; no conclusion on this point could be drawn from the 1-MeV irradiated p-i-n diodes due to the very rapid disappearance of the divacancy.

The sample dependence of the divacancy annealing has been previously reported[26] in a study showing that the divacancy annealed more rapidly in Czochralski silicon than in float zoned. This effect was explained by proposing that the oxygen atoms in the former acted as efficient sinks for vacancies dissociating from the divacancy. This is also likely to be the explanation for the faster anneal of the divacancy in the p-i-n sample. The variation in divacancy annealing rate with irradiation energy could be a genuine energy effect of, as yet, unexplained origin, or it could be a reflection of the effect of different background total trap concentrations. Further study is required to resolve this point.

As shown in Fig. 12, and also discussed in this and the preceding section, significant concentrations of two different defects appeared in the p-i-n and Schottky barrier samples, respectively, during annealing at temperatures of 277 °C and above. Two higher-order oxygen-vacancy complexes have been reported by Lee and Corbett[33] to anneal in over this temperature range. They were identified as a trivacancy + oxygen and a divacancy + 2 oxygen, with the former being more abundant. Although these are likely candidates for the centers observed in this study, the mechanisms which predispose the formation of one rather than the other in the devices studied are not clear.

VI. CONCLUSION

A study has been made of defect creation and annealing in high-resistivity float-zoned n-type silicon of the type commonly used for power devices. The power device processing schedule, involving many hours diffusion in oxygen at temperatures in excess of 1200 °C, has been found to appreciably modify the internal defect reactions as a result of the increased oxygen content of the material. This was particularly noticeable when comparing the fully fabricated p-i-n diodes with Schottky barrier diodes made on otherwise unprocessed substrates. In particular, the formation of two vacancy-related complexes (one of which was the E center) were suppressed in the oxygen-rich p-i-n samples, although there was no difference in the production rate of the oxygen-related center (the A center) between the high and low oxygen content material. It would thus appear that the oxygen content in float-zoned material (10^{15}–10^{16} cm^{-3}) is sufficient to support the creation of A centers, at least up to densities of 5×10^{13} cm^{-3}. The higher oxygen content in the p-i-n samples, while producing no more A centers, would appear to act as sinks for vacancies or as recombination sites for Frenkel pairs.

The annealing results were also found to be a function of sample type and were of considerable complexity, displaying a number of hitherto unreported features. In particular, differences in the annealing characteristics of both the divacancy and the A center were noted between the p-i-n samples and the Schottky barrier samples, and in the case of the divacancy, the annealing rate was also a function of the irradiation energy. In contrast to the defect creation effects, some of these differences could not be correlated with the increased oxygen content of the p-i-n samples. This was also true of the major annealing induced centers: different centers were seen to anneal into Czochralski samples and the float-zoned p-i-n samples (differences were, of course, also seen between the p-i-n and Schottky barrier samples in this respect). Further study is required to satifactorily resolve some of these features.

The samples in this study, irradiated with 1- and 12-MeV electrons and with Co^{60} γ rays, provided convenient vehicles for determining the centers responsible for recombination lifetime control. The conclusion drawn was that, while the lifetime changes could not be satisfactorily explained in terms of either the A center or the divacancy alone being the dominant recombination center, if both centers were assumed to act in parallel, then all the results could be placed upon a common curve, which simply related changes in switching speed to the total concentration of divacancies and A centers.

Finally, results were presented on the electrical characterization of the major radiation-induced defects. By extracting values of the vibrational entropy changes from these data, good consistency was found between the nature of the bonding states inferred from these electrical measurements and that previously determined by ESR measurements.

ACKNOWLEDGMENTS

The authors would like to thank Dr. M. Moore and P. Green of Mullard, Ltd., Hazel Grove, for the supply of the p-i-n samples. Thanks are also due to J. A. G. Slatter for making available the diode switching program, developed by himself and Dr. J. P. Whelan.

[1] R. Rai-Choudhury, J. Bartko, and J. E. Johnson, IEEE Trans. Electron Devices **ED-23**, 814 (1976).
[2] R. O. Carlson, Y. S. Sun, and H. B. Assalit, *ibid.* **ED-24**, 1103 (1977).
[3] A. O. Evwaraye and B. J. Baliga, J. Electrochem. Soc. **124**, 913 (1977).
[4] S. D. Brotherton and P. Bradley, *Semiconductor Silicon*, edited by H. Huff, R. J. Kriegler, and Y. Takeishi (Electrochemical Society, New York, 1981), p. 779.
[5] G. D. Watkins, J. W. Corbett, and R. M. Walker, J. Appl. Phys. **30**, 1198 (1959).
[6] G. D. Watkins and J. W. Corbett, Phys. Rev. **121**, 1001 (1961).

[7]J. W. Corbett and G. D. Watkins, *ibid.* **138**, 555 (1965).
[8]L. C. Kimerling, Inst. Phys. Conf. Ser. **31**, 221 (1977).
[9]D. Bielle-Daspet, Solid-State Electron. **16**, 1103 (1973).
[10]H. J. Hrostowski and R. H. Kaiser, Phys. Rev. **107**, 966 (1957).
[11]R. A. Logan and A. J. Peters, J. Appl. Phys. **30**, 1627 (1959).
[12]J. Crank, Mathematics of Diffusion, OUP (1956).
[13]W. Kaiser, Phys. Rev. **105**, 1751 (1957).
[14]B. Whittaker, *Radiation Dosimetry Manual* (Dekker, New York, 1960), p. 363.
[15]D. V. Lang, J. Appl. Phys. **45**, 3023 (1974).
[16]G. D. Watkins, J. R. Troxell, and A. P. Chatterjee, Inst. Phys. Conf. Ser. **46**, 16 (1979).
[17]A. O. Evwaraye and E. Sun, J. Appl. Phys. **47**, 3776 (1976).
[18]S. D. Brotherton and J. Bicknell, *ibid.* **49**, 667 (1978).
[19]S. D. Brotherton, P. Bradley, and J. Bicknell, *ibid.* **50**, 3396 (1979).
[20]H. G. Grimmeiss, E. Janzen, and B. Skarstam, *ibid.* **51**, 4212 (1980).
[21]S. D. Brotherton, M. J. King, and G. J. Parker, *ibid.* **52**, 4649 (1981).
[22]H. G. Grimmeiss, E. Janzen, and B. Skarstam, *ibid.* **51**, 3740 (1980).
[23]J. E. Lowther, J. Phys. C **13**, 3681 (1980).
[24]J. A. Van Vechten and C. D. Thurmond, Phys. Rev. B **14**, 3539 (1976).
[25]O. Engstrom and A. Alm, Solid-State Electron. **21**, 1571 (1978).
[26]L. J. Cheng, J. C. Corelli, J. W. Corbett, and G. D. Watkins, Phys. Rev. **152**, 761 (1966).
[27]G. D. Watkins and J. W. Corbett, *ibid.* **134**, 1359 (1964).
[28]R. H. Kingston, Proc. IRE **42**, 829 (1954).
[29]J. A. G. Slatter and J. P. Whelan, Solid-State Electron. **23**, 1235 (1980).
[30]S. D. Brotherton and P. Bradley, *ibid.* **25**, 119 (1982).
[31]P. I. Lugakov, V. D. Tkachev, and V. V. Shusha, Sov. Phys. Semicond. **13**, 514 (1979).
[32]J. W. Corbett, G. D. Watkins, R. M. Chrenko, and R. G. McDonald, Phys. Rev. **121**, 1015 (1961).
[33]Y. H. Lee and J. W. Corbett, Phys. Rev. B **13**, 2653 (1976).